frontiers | Frontiers in Earth Science

TYPE Original Research
PUBLISHED 24 August 2023
DOI 10.3389/feart.2023.1192269

OPEN ACCESS

EDITED BY
Wenzhuo Cao,
Imperial College London,
United Kingdom

REVIEWED BY
Yi Xue,
Xi'an University of Technology, China
Xiaoping Zhou,
Chongqing University, China
Jie Liu,
Hunan Institute of Engineering, China

*CORRESPONDENCE
Jun Du,
dujun0605@126.com

RECEIVED 23 March 2023
ACCEPTED 09 August 2023
PUBLISHED 24 August 2023

CITATION
Du J, Shen X, Li C, Zhu W and Feng G (2023), Effect of dry-wet cycles on the strength and deformation of the red-bed rockfill material in western Yunnan. *Front. Earth Sci.* 11:1192269. doi: 10.3389/feart.2023.1192269

Effect of dry-wet cycles on the strength and deformation of the red-bed rockfill material in western Yunnan

Jun Du*, Xinggang Shen, Chenchen Li, Weiwei Zhu and Guojian Feng

College of Architecture and Civil Engineering, Kunming University, Kunming, China

Introduction: The shear strength deterioration of red-bed rockfill under the dry-wet cycle is the key factor affecting the slope stability of accumulation body. Studying the strength deterioration law and deterioration mechanism of red-bed rockfill can provide theoretical support for slope stability control.

Methods: Through the disintegration resistance test of argillaceous siltstone rockfill in Lanping lead-zinc Mine, the disintegration characteristics of red-bed soft rock were studied. The effects of the number of dry-wet cycles on the cohesion, internal friction angle, shear dilation rate and shear modulus of the red-bed rockfill were investigated by using a dry-wet cycle shear tester to conduct shear tests on the reduced scale graded soil material, and the strength deterioration mechanism of the soils was revealed from the perspective of meso-structure.

Results: The results showed that argillaceous siltstone was rich in clay minerals and produces strong disintegration when exposed to water. The disintegration process could be divided into three stages: massive disintegration stage, transitional stage and stabilization stage. With the accumulation of dry-wet cycles, the shear dilation rate and shear modulus of the argillaceous siltstone rockfill gradually decrease, and the shear failure developed gradually from strain hardening to shear plastic flow, and the characteristic of weak stress softening occurred. After eight dry-wet cycles, the cohesion and internal friction angle of argillaceous siltstone rockfill materials decreased by 89.87% and 18.94%, respectively, indicating a higher effect on the cohesion than on the internal friction angle.

Discussion: The thickening of the bound water between the fine particles on the shear surface, the weakening of the coarse particle attachment, and the increase in the number of directionally arranged fine particles were the main reasons for the continuous deterioration of the soil strength.

KEYWORDS

argillaceous siltstone, rockfill material, dry-wet cycle, disintegration, deterioration of strength

1 Introduction

The red Jurassic and Cretaceous strata are widely distributed in Yunnan, China. Bounded by the Erhai-Honghe Fault, the eastern and western parts are called the Central Yunnan Red Bed and the Western Yunnan Red Bed, respectively, due to their different phase zones. The Western Yunnan Red Bed is mainly composed of inland lacustrine formations. Its lithology is clastic sedimentary rocks such as mudstone, siltstone, argillaceous siltstone, and sandstone (Luo et al., 2003). These rocks are rich in clay minerals, poorly permeable, hydrophilic, easily swollen, and disintegrated by water, with a large softening property (Zhang et al., 2017; Zhang et al., 2019; Zeng et al., 2021). In recent years, the continuous exploitation of mineral resources in western Yunnan has led to the gradual excavation and stripping of red-bed rocks. As a result, large amounts of waste rock materials are frequently deposited around, forming large loose accumulation slopes. Under frequent rainfall infiltration and evaporation, the mechanical properties of the rockfill material inevitably deteriorate (Oliveira et al., 2021; Wen and Yuan, 2022; Xue et al., 2023), reducing the stability of the slope (Pan et al., 2020; Nguyen et al., 2023) and aggravating its long-term deformation (Zhou et al., 2014; Cook et al., 2023; Wei et al., 2023). In order to analyze the stability of loose accumulation slope, it is of great importance to study the performance deterioration of red-bed rockfill materials in western Yunnan under alternating wet and dry environments.

Loose accumulations formed by geological tectonic movements or human engineering activities are widely distributed in nature. These geological bodies have a typical soil-rock binary mixed structure, and no single part can represent the characteristics of the entire body (Wang et al., 2012; Zhou et al., 2018). The particle gradation composition, the contact type of the blocks, and the mineral composition of the parent rock significantly affect the strength and deformation of the soil (Cavarretta et al., 2010; Yuan et al., 2018; Pham et al., 2022; Xue et al., 2023). Firstly, the particle composition of the rockfill material is complex. The percentage of coarse and fine particles and the size of the blocks are constantly changing in space. The contact interaction between soil particles is exceptionally significant in the variation of soil grading, and the different contact relationships between particles control the ability of the soil to resist deformation and damage (Wu et al., 2020; Tran et al., 2021). With the increased size of block stones and increased block stone content in the soil, the squeezing and interlocking between the particles are continuously enhanced, and the shear damage resistance of the soil is significantly increased. However, the increase in block content can also cause massive soil pores to penetrate each other, weakening the resistance of the soil against infiltration deformation damage. Secondly, the mechanical properties of rockfill materials are mainly shear yielding. These materials are highly susceptible to particle breakage under stress concentration (Li et al., 2019; Zhou et al., 2019; Wu et al., 2021), with obvious shear dilation characteristics during shear deformation (Chen et al., 2018; Ahmed et al., 2023). The fragmentation of the block particles changes the original particle contact relationship in the soil, reducing the interlocking force and friction strength between the particles. As the stress increases, relative sliding continuously occurs among the yield-ruptured soil particles, resulting in irrecoverable plastic deformation of the soil body and damage. Therefore, a series of granular material mechanical behaviors in the shear deformation of rockfill materials make their shear strength properties exceptionally complex, which requires continuous in-depth research.

In addition, the mechanical properties of the soil are closely related to environmental conditions. The deterioration of rockfill materials under dry-wet cycles reduces their shear strength and deformation modulus, which is the main cause of excessive deformation and instability of high-fill slopes (Silvani et al., 2008; Peng and Zhang, 2012; Zhou et al., 2019; Wu et al., 2021). In order to analyze the strength deterioration characteristics of soil, several scholars have conducted experimental studies on the strength and deformation of soil under dry-wet cycles (Rasul et al., 2018; Zhou et al., 2019; Xu et al., 2021; Li et al., 2022; Abbas et al., 2023). The triaxial wetting deformation test of rockfill materials showed that particle water immersion disintegration and fragmentation are the main reasons for increased soil deformation (Wei and Zhu, 2006; Jia et al., 2019; Zhang and Zhou, 2020). The degree of particle fragmentation increased with the accumulation of dry-wet cycles (Zhang et al., 2015). The deterioration of rockfill material strength properties is mainly because the rock is rich in hydrophilic clay minerals (Jia et al., 2018). The block particles constantly crack in multiple wet and dry deformations, reducing the strength of the parent rock and weakening the shear strength of the soil. However, the stress levels in the existing experimental studies of rockfill materials undergoing wet-dry cycles are usually inconsistent with reality. Limited by the test conditions, the dry-wet cycle deterioration test is usually performed by soaking and air-drying the stone particles several times before loading them into the test machine. In reality, the fill slope only experiences rainfall infiltration and evaporation changes after completing soil accumulation, and the soil dry-wet cycle is completed under a specific consolidation stress state. Therefore, it is necessary to improve the existing geotechnical test equipment to realize the dry-wet cycle after sample preparation, thus revealing the deterioration characteristics of rockfill materials under consolidation stress conditions.

The strength deterioration of red-bed rockfill materials under alternating dry-wet environments is the key factor affecting the stability of loose accumulation slope. In order to study the strength deterioration characteristics and mechanisms of red-bed rockfill materials under dry-wet cycles, argillaceous siltstone rockfill materials from Lanping lead-zinc mine was selected as the research object. The disintegration characteristics, strength degradation, and deformation damage of rockfill materials were studied by water immersion disintegration test and dry-wet cycle shear test, and the mechanism of strength degradation of rockfill materials was revealed from the perspective of meso-structure. The research results could reveal the deterioration characteristics of red-bed rockfill from macro-meso structure, provide reasonable soil mechanical analysis parameters for mine dump heightening and expansion and slope design, and provide certain scientific guidance for the safety risk management of dump slope.

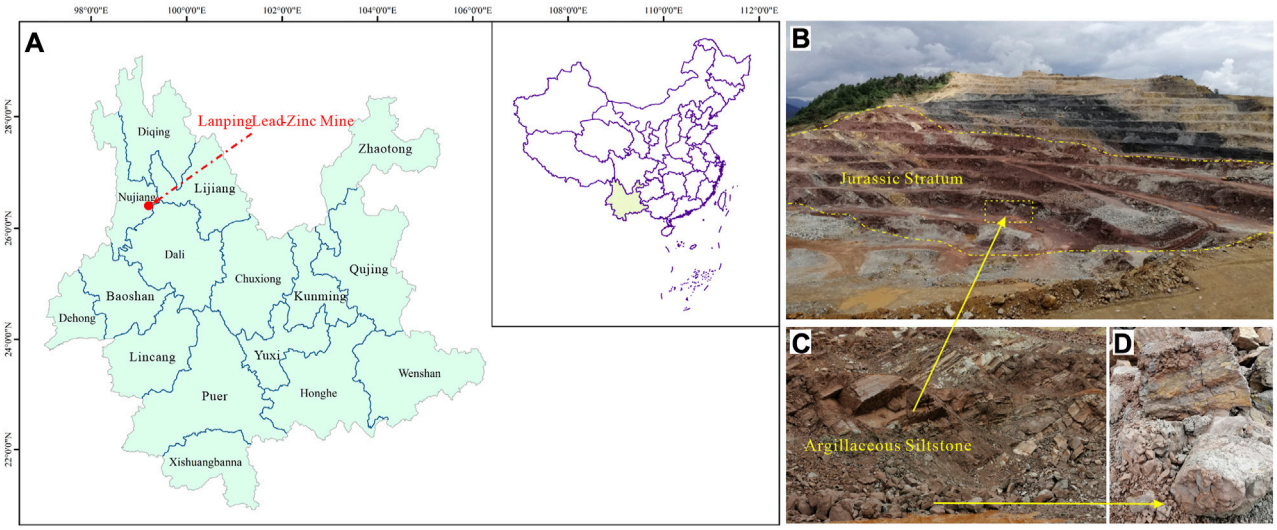

FIGURE 1
The location of Lanping lead-zinc mine. **(A)** Geographical location. **(B)** Mine overview. **(C)** Argillaceous siltstone. **(D)** Rock under wetting-drying cycles.

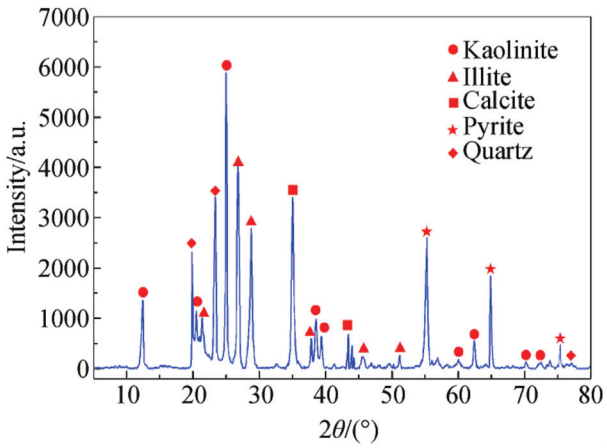

FIGURE 2
Mineralogical compositions of the argillaceous siltstone.

2 Performance deterioration test for rockfill materials during dry-wet cycles

2.1 Basic characteristics of the test material

The test material is argillaceous siltstone rockfill material, which was taken from the dumping site of Lanping lead-zinc mine in Yunnan Province (N26°24′, E99°25′). The waste rock of the dumping site mainly consists of purplish-red argillaceous siltstone of the Middle Jurassic Huakaizuo strata (J_2h) excavated from the open mine, as shown in Figure 1. The mining area is located on the southwest border of China, falling into the low-latitude mountain monsoon climate zone, with the vertical distribution of three-dimensional climate characteristics. The annual average temperature is 7°C, the annual rainfall is 1,002.4 mm, the annual average sunshine hour is 2008.7 h, and the annual average evaporation is 1,063 mm. Therefore, the rockfill materials in the dumping field are significantly affected by the alternating dry and wet climate. The frequent dry-wet cycles exacerbate the performance deterioration of the rockfill material, which can easily induce landslide geological hazards.

Figure 2 shows the mineral composition of the argillaceous siltstone obtained through X-ray diffraction analysis. The mineral composition of the argillaceous siltstone and its content are: quartz 22%, kaolinite 42%, illite 20%, calcite 11%, and pyrite 6%. The mineral composition of more than 60% indicates a high content of clay minerals.

Figure 3 shows the microstructure of the argillaceous siltstone by a scanning electron microscope (SEM). The SEM image of the rock at 500 times magnification (Figure 3A) reveals that the microstructure unit is dominated by agglomerated aggregates with large particle sizes. The contact between the particles is mainly surface-to-surface, which belongs to the laminating structure. Fine viscous particles are scattered on the surface of the agglomerates and gathered into clusters, and the geometric size, shape, and orientation of the particles differ significantly. Figures 3B, C show the SEM images of the rock at 2000 and 4,000 times magnification, respectively, clearly displaying the clay particles and quartz particles inside.

The rockfill material was sieved on site, and the dividing particle size of coarse and fine particles was 5 mm (Wang et al., 2009), i.e., particles below 5 mm were fine particles, and those beyond 5 mm were coarse particles. The coarse grain contents were expressed as P_5. Then, the equivalent alternative scaling was performed for field grading of test soil materials according to Eq. 1. The composition of the test soil grade is shown in Figure 4.

$$P_{5i} = P_{05i} \cdot \frac{P_5}{P_5 - P_0} \tag{1}$$

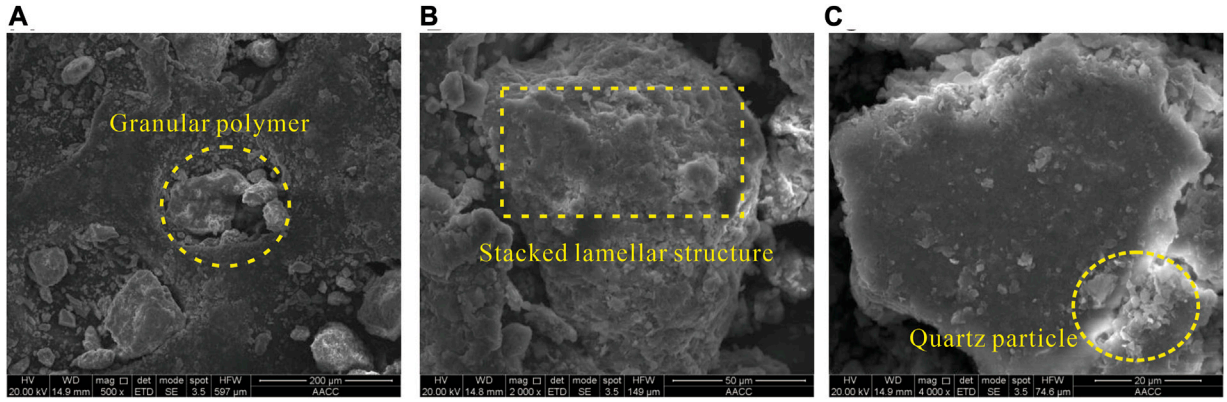

FIGURE 3
Microscopic image of the argillaceous siltstone. **(A)** 500 times. **(B)** 2000 times. **(C)** 4,000 times.

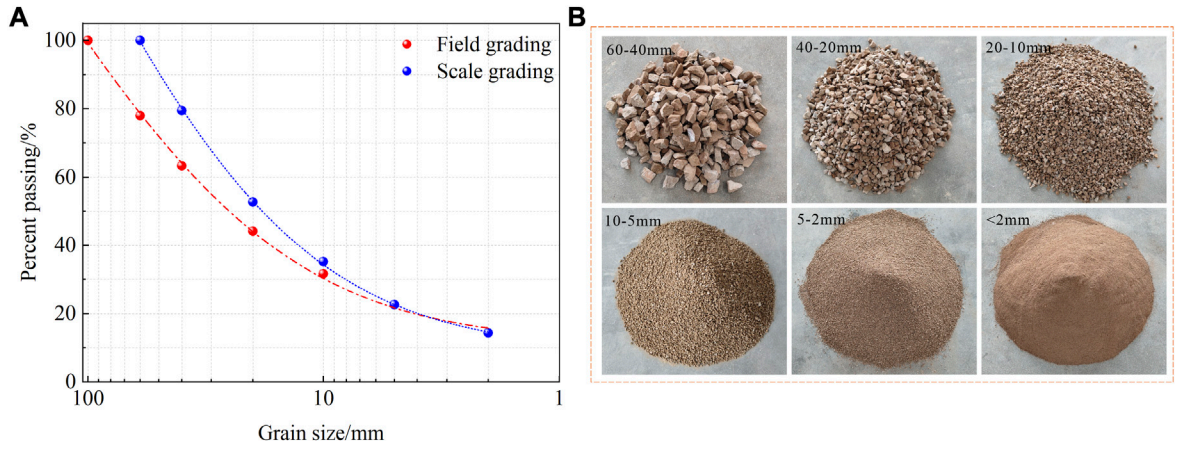

FIGURE 4
Particle grading components. **(A)** Grain size distribution. **(B)** Different grain groups of soil materials.

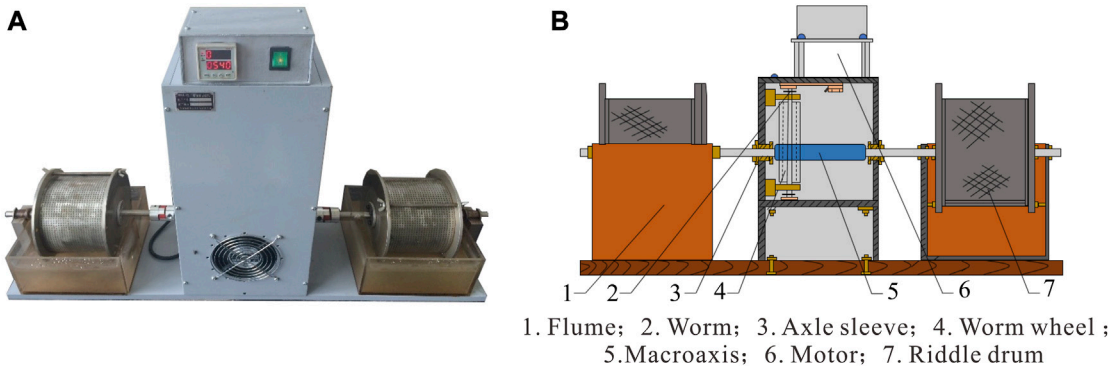

FIGURE 5
Disintegration resistance test instrument. **(A)** Instrument. **(B)** Instrument construction.

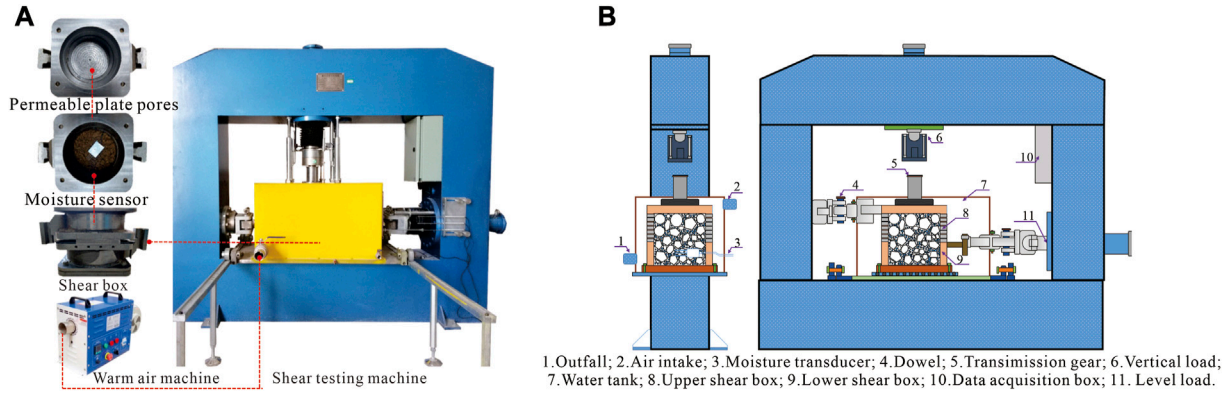

FIGURE 6
Shear testing machine of coarse-grained soil. **(A)** Test machine. **(B)** Machine construction.

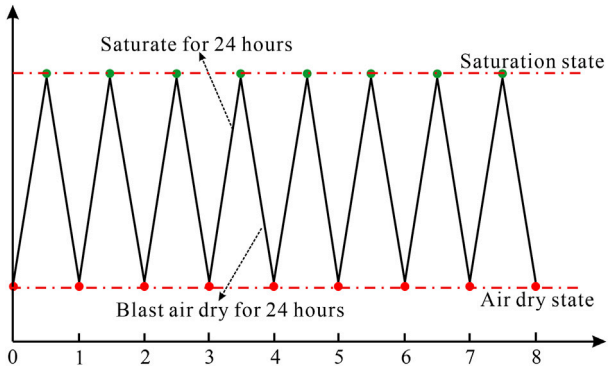

FIGURE 7
Dry-wet cycles method.

Where P_5 is coarse grain contents (%), P_{5i} is the content of a particle group with a particle size greater than 5 mm after scaling (%), P_{05i} is the content of a particle group with a particle size greater than 5 mm before scaling (%), and P_0 is percentage of particle mass with a particle size greater than 60 mm.

2.2 Disintegration resistance test

Figure 5 shows the disintegration resistance test apparatus for clay rocks. The coarse particles greater than 5 mm were weighed according to the composition of the test soil grade and loaded into the drum sieve of the disintegration resistance tester at dry room temperature. Referring to the *Standard for Rock Physical and Mechanical Properties Testing Method* (DZ/T 0276.9–2015), the drum sieve was placed into the water tank, followed by the injection of pure water to keep the water level about 20 mm below the rotation axis. Afterward, the drum sieve was rotated at r/min for 10 min before removing the test soil and drying at a constant temperature of 105–110°C for 24 h. The dried soil materials were passed through 40, 20, 10, and 5 mm sieves, weighed, and recorded to obtain the particle size distribution. The above test procedure was considered as one disintegration. The coarse particles greater than 5 mm were loaded into the sieve again, and the above test process was repeated eight times.

TABLE 1 Dry-wet cycle shear test scheme of rockfill material.

No	Dry-wet cycle *n*	Normal load σ/kPa			
T1	0	200	400	600	800
T2	1	200	400	600	800
T3	2	200	400	600	800
T4	4	200	400	600	800
T5	6	200	400	600	800
T6	8	200	400	600	800

2.3 Dry-wet cycle direct shear test

Figure 6 shows the DJH30 dry-wet cycle shear tester for coarse-grained soils. The tester is equipped with a computerized automatic data acquisition and processing system, allowing the collection and storage of load and displacement and the automatic control of the vertical load, horizontal load, and shear rate. The shear box of the tester is Φ300 × 240 mm, which can be used to determine the shear strength of coarse-grained soil with a grain diameter of less than 60 mm. Since the tester has a saturated water tank and a blower, the dry-wet cycle can be achieved inside the tester. When the specimen is prepared again after the wet-dry cycle outside the testing machine, the manual interference with the test soil can be overcome. The dry-wet cycle shear test path is designed by incorporating the functional characteristics of the test machine, as shown in Figure 7. The protocol of the dry-wet cycle shear test is shown in Table 1.

Referring to the *S. for Geotechnical Testing Method* (GB/T50123-2019), the test soil material was air-dried and sieved, and the specimens were prepared according to the moisture content of 4.32% and density of 2.05 g/cm^3 to complete the dry-wet cycle shear test. The main test steps are as follows.

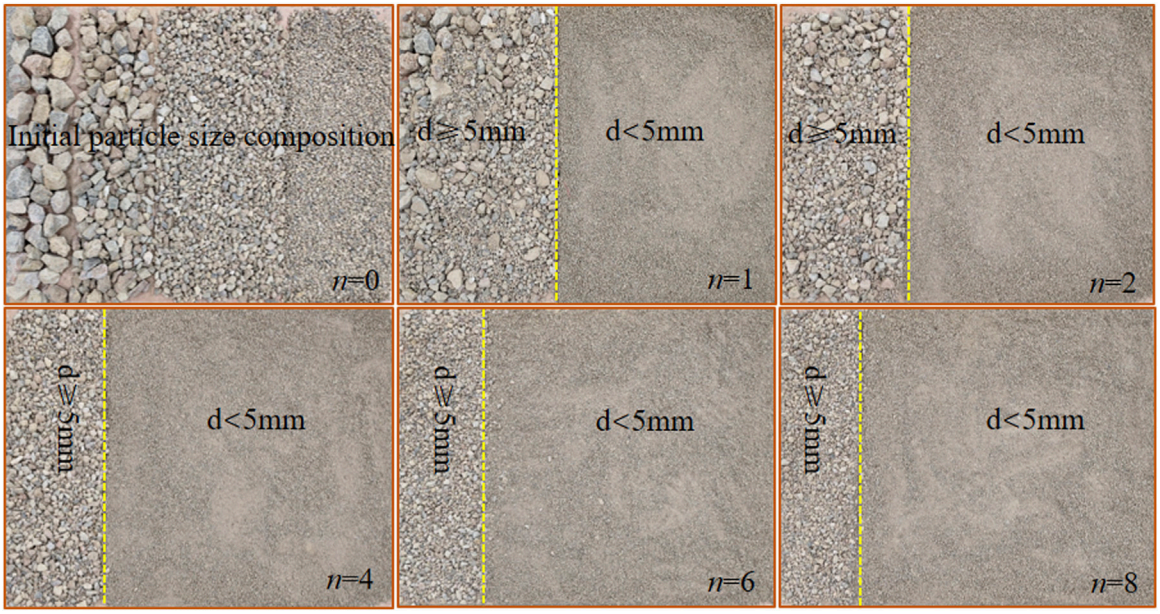

FIGURE 8
Rockfill disintegration resistance test phenomenon.

(1) According to the composition of the soil scale grading, three parts of air-dried soil are weighed and properly mixed after adding an appropriate amount of water. Afterward, three parts of the materials are filled into the shear box sequentially according to the density control conditions, and the layers are chiseled to reduce the effect of anisotropy.

(2) The dry-wet cycle process is realized for the prepared specimens. Firstly, the water tank is filled. Water along the permeable plate pores at the bottom of the shear box gradually penetrates upward to the interior of the specimen, allowing the specimen to be completely saturated. The time of saturation is 24 h. Then, the water tank is emptied, and the pore water inside the specimen is gradually emptied under differential pressure. In order to make the soil particles inside the sample fully dry, a blower is used to blow continuously inside the sample for 24 h, and the soil sample is regarded as dry when the water content is below 5% measured by the built-in moisture sensor in the sample. When the moisture content of the soil sample is below 5% and the blast drying is less than 24 h, it is still necessary to continue to blast for 24 h. The above operation is a dry-wet cycle. Finally, dry-wet cycles corresponding to each specimen are completed according to the test protocol.

(3) Specimens that have completed the wet-dry cycles are subjected to the direct shear test. The test loading is strain-controlled, and the shear rate is 1 mm/min. When the shear displacement reaches 15% of the specimen size, the specimen is considered to be shear damaged. In the test, the specimen shear box is round and the diameter is 300 mm. Therefore, when the shear displacement of the sample reaches 45 mm, the sample is shear damaged and the test is terminated.

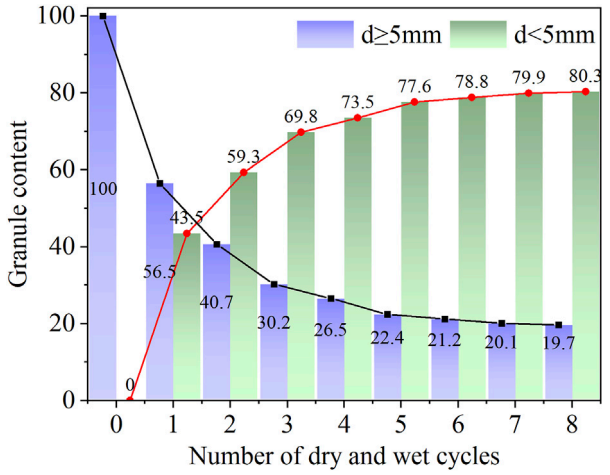

FIGURE 9
Change characteristics of disintegration under dry-wet cycles.

3 Analysis of disintegration resistance test results

3.1 Disintegration phenomenon

In the disintegration test, the test soil material disintegrates with the increasing number of wet-dry cycles *n*, as illustrated in Figure 8. As the argillaceous siltstone is rich in clay minerals, it reacts vigorously with water, and the blocks show different degrees of cracking along the primary structural surface. The large blocks gradually crack into disintegrated materials with

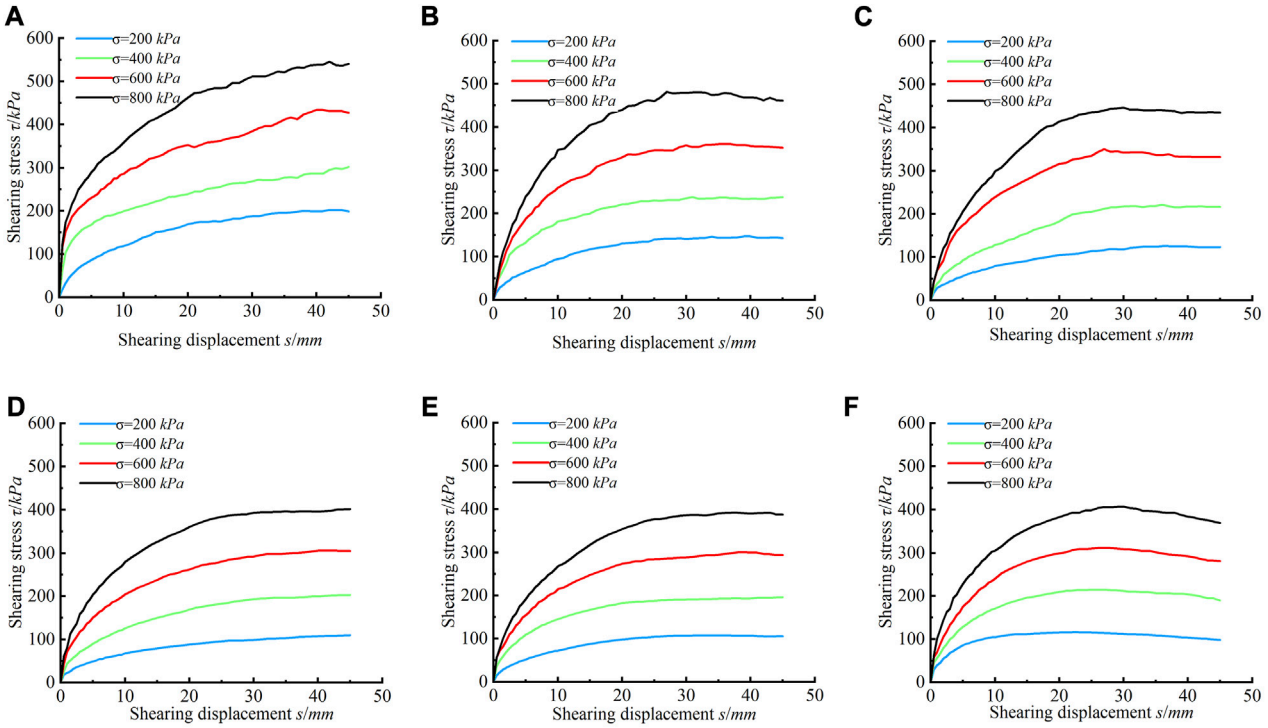

FIGURE 10
Shear stress-displacement curve. **(A)** N = 0 **(B)** n = 1 **(C)** n = 2 **(D)** n = 4 **(E)** n = 6 **(F)** n = 8.

smaller particle sizes. When comparing the soil gradation in the initial stage of the test, it can be seen that when n=1 (wet-dry cycle for 24 h), the content of particles larger than 5 mm is significantly reduced in the test soil material, and the roundness of the block increases. With the accumulation of dry-wet cycles, the blocks are further cracked, and the content of disintegrated materials is significantly increased. When a certain number of wet-dry cycles are reached, the disintegration rate of blocks with better integrity slows down, and the content of disintegrated material gradually stabilizes.

3.2 Content variation of disintegrated materials

The content variations of coarse particles ($d \geq 5$ mm) and disintegrated materials ($d < 5$ mm) with dry-wet cycles are shown in Figure 9. According to the disintegration degree of the coarse particles in Figure 9, the disintegration process can be divided into three stages.

(1) Massive disintegration stage ($n \leq 2$). In this stage, the rockfill material is massively disintegrated in water. With the increase of n, the content of coarse particles significantly decreases, and the content of disintegrated materials significantly increases.
(2) Transitional stage ($2 < n \leq 4$). In this stage, the disintegration rate of coarse particles in water slows, with less increase in disintegrated material content. The block is in the transitional stage from vigorous disintegration to disintegration completion.
(3) Stabilization stage ($n > 4$). After the disintegration of coarse particles in water reaches a certain value, it is difficult for coarse particles to crack, with almost no changes in the content of the disintegrated material. At this point, the soil disintegration is completed and is in the stabilization stage.

Taking the test soil material before dry-wet cycles as the benchmark, the coarse particle content decreases by 59.3% in the massive disintegration stage, further decreases by 18.3% in the transitional stage, and decreases by only 2.7% in the stabilization stage. The coarse particle content is 19.7% when n = 8. This result indicates that with the accumulation of wet-dry cycles, the coarse particle content of the argillaceous siltstone rockfill material decreases, and the block disintegration gradually slows down and finally stabilizes.

4 Analysis of dry-wet cycle shear test results

4.1 Soil strength properties

4.1.1 Shear stress-displacement characteristics

The shear stress-displacement curves of argillaceous siltstone rockfill materials under dry-wet cycles are shown in Figure 10. It can be seen that there are no significant peaks, and the changing patterns of the test curves corresponding to different numbers of wet-dry cycles are different. When the number of dry-wet cycles is 0, the shear stress increases with the increase of shear displacement. The

TABLE 2 Deterioration of shear strength of rockfill material under dry-wet cycles.

Dry-wet cycle *n*	σ=200 kPa		σ=400 kPa		σ=600 kPa		σ=800 kPa	
	τ/kPa	*δ*/%	*τ*/kPa	*δ*/%	*τ*/kPa	*δ*/%	*τ*/kPa	*δ*/%
0	198.37	0	302.16	0	427.54	0	540.83	0
1	142.18	28.33	237.46	21.41	352.17	17.63	461.09	14.74
2	122.98	38.01	215.97	28.52	331.92	22.37	434.99	19.57
4	110.05	44.52	203.17	32.76	305.49	28.55	402.31	25.61
6	105.28	46.93	195.95	35.15	293.92	31.25	387.87	28.28
8	97.99	50.61	189.36	37.33	281.44	34.17	369.19	31.74

variation curve is not smooth with some fluctuations, especially during soil shear yielding and damage stages. The reason is that the coarse particles that have not yet disintegrated are closely squeezed and interlocked. With the rapid increase of the shear stress, the local stress exceeds the particle contact strength, resulting in particle cracking. The strain energy stored in the soil due to particle squeezing and interlocking is rapidly released, which causes fluctuations in shear stress. Subsequently, the soil particles are arranged in a new orientation under pressure. The particles on the shear surface interlock and roll again as shear stress returns. This process is repeated until shear damage to the soil sample occurs. The soil shear stress-deformation relationship during this process exhibits a hardening characteristic. When the number of dry-wet cycles is 1 and 2, the coarse particles show strong disintegration due to immersion. The number of coarse particles squeezing and interlocking each other decreases, and the soil shear stress fluctuation and hardening characteristics gradually weaken with the development of shear deformation. When the number of dry-wet cycles is 4, the disintegration of coarse particles is basically completed. The content of fine particles sharply increases, and coarse particles are mostly suspended in fine particles. During the shear deformation of the soil, the interlocking and rolling among particles continuously disappear, and the particle contact is mostly adhesion and friction of fine particles. With the development and expansion of cracks on the shear surface, the soil shear stress slowly increases and tends to be constant until the occurrence of plastic flow damage. When the number of wet-dry cycles is 6 and 8, the shear-plastic flow characteristics of the soil become increasingly significant after yielding, accompanied by a weak stress softening. Based on the above results, the shear characteristics of argillaceous siltstone rockfill material under dry-wet cycles are closely related to the disintegration characteristics of coarse particles. With the accumulation of dry-wet cycles, the soil shear damage gradually develops from strain hardening to shear plastic flow, exhibiting specific stress softening characteristics.

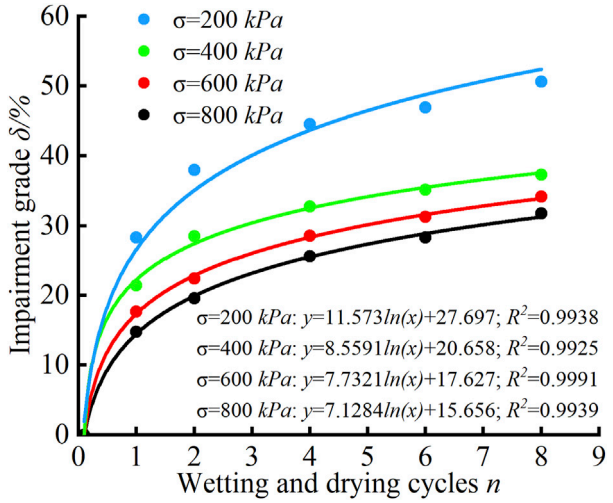

FIGURE 11
Deterioration degree of shear strength under dry-wet cycles.

4.1.2 Shear strength deterioration characteristics

Since there is no apparent peak stress for soil shear damage in the test, the strength corresponding to 45 mm of shear displacement is taken as the shear strength τ of the soil according to the *S. for Geotechnical Test Method* (GB/T50123-2019). To analyze the degradation of soil shear strength under dry-wet cycles, the degradation of soil shear strength δ is defined as follows:

$$\delta = \frac{\tau_0 - \tau_n}{\tau_0} \times 100\% \quad (2)$$

where τ_0 is the soil shear strength under 0 dry-wet cycles (kPa); τ_n is the soil shear strength under different numbers (n = 1, 2, 4, 6, 8) of dry-wet cycles (kPa).

The shear strength deterioration of the soil obtained by Eq. 2 is shown in Table 2.

It can be seen from Table 2 that the shear strength of the soil deteriorates significantly under dry-wet cycles, and the degree of strength deterioration varies under different vertical consolidation stresses. The degradation of soil shear strength under the dry-wet cycles decreases with the increase of vertical consolidation stresses, indicating the suppressive effect of vertical consolidation stresses on the degradation of soil strength in dry-wet cycles. After eight wet-dry cycles, the shear strength of the soil deteriorates by 50.61% at consolidation stress of 200 kPa, while its deterioration is 31.74% at 800 kPa.

TABLE 3 Shear strength parameters of soil under different dry-wet cycles.

Dry-wet cycle *n*	Shear strength parameters	
	Cohesion *c* (kPa)	Internal friction angle (°)
0	79	30.1
1	30	28.2
2	13.5	27.7
4	10.5	26.1
6	9	25.3
8	8	24.4

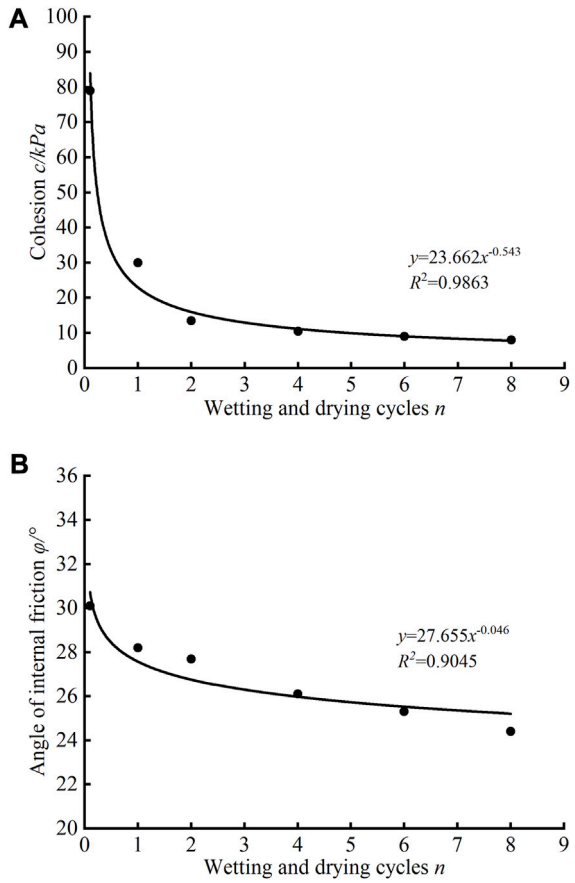

FIGURE 12
Deterioration characteristics of shear strength index under dry-wet cycles. **(A)** Cohesion. **(B)** Angle of internal friction.

Figure 11 shows the variation of soil shear strength with dry-wet cycles under different vertical consolidation stresses. To simplify the fitting function, 0.1 was used to represent 0 dry-wet cycles. It can be seen that the shear strength degradation of soil under the same vertical consolidation stress conforms to the logarithmic function, with significant non-uniformity under dry-wet cycles, which is closely related to the soil disintegration characteristics. During the massive disintegration stage ($n \leq 2$), the degradation of soil shear strength under dry-wet cycles is significantly increased. During the transitional stage ($2 < n \leq 4$), the disintegration of coarse soil particles in water slows down. The soil structure is relatively stable, and the rate of shear strength deterioration decreases. During the stabilization stage ($n > 4$), the block disintegration tends to be stable, with rare cracks generated by the coarse particles. The disintegrated material content remains almost unchanged, and the soil shear strength deterioration rate gradually reaches the limit value.

4.1.3 Variation pattern of the shear strength index

To analyze the variation pattern of soil shear strength index under dry-wet cycles, the Mohr-Coulomb criterion was used to fit σ and τ.

$$\tau = \sigma \tan \varphi + c \tag{3}$$

where σ and τ are the normal stress (kPa) and shear stress (kPa) on the soil shear plane. c and φ are the cohesion (kPa) and internal friction angle (o), respectively.

The shear strength index of the soil under different dry-wet cycles obtained by Eq. 3 is shown in Table 3.

Figure 12 shows the variation of soil shear strength with dry-wet cycles. Under dry-wet cycles, the degradations of soil cohesion and internal friction angle are consistent, both showing the trends of first decreasing and then stabilizing. However, the degradation of the cohesion is significantly larger than that of the internal friction angle. After one wet-dry cycle, the cohesive force and internal friction angle decrease by 62.03% and 6.32%, respectively. After four wet-dry cycles, the cohesion and internal friction angle decrease by 86.71% and 13.29%, respectively. After eight wet-dry cycles, the cohesion and internal friction angle decrease by 89.87% and 18.94%, respectively. The reason is that the cohesion and the internal friction angle of the rockfill material are composed of the interlocking force and friction strength between soil particles. Although the inter-particle friction strength decreases with the decreasing number of block particles, the broken particles still have a certain friction strength under the consolidation stress, leading to a relatively small internal friction angle.

Assuming that the damage to the soil by dry-wet cycles is a continuous process, the damage evolution equation for the shear strength parameters of the soil can be established. Statistical analysis reveals that the deterioration trend of shear strength parameters of argillaceous siltstone rockfill materials can be better fitted by the following power functions:

$$c = 23.662n^{-0.543}, \quad R^2 = 0.975 \tag{4}$$

$$\varphi = 27.665n^{-0.046}, \quad R^2 = 0.9029 \tag{5}$$

4.2 Soil deformation characteristics

4.2.1 Shear dilation rate

In addition to shape changes, volume changes also occur during soil shear damage. The volume dilation and volume contraction of soil due to shear stress is referred to as shear dilation (Huang et al., 2016). In the direct shear test, the upward vertical displacement of the soil indicates shear dilation, and the downward vertical

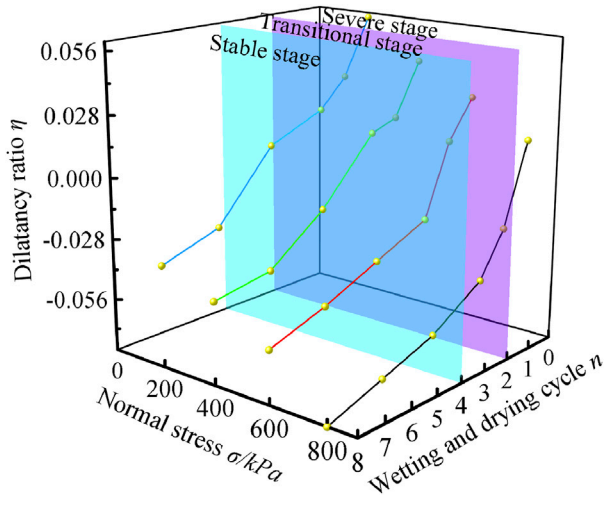

FIGURE 13
Curves of shear dilation rate under dry-wet cycles.

displacement indicates shear contraction. The shear dilation rate η for soil shear damage can be calculated based on Eq. 6:

$$\eta = \tan\psi = \frac{d\varepsilon_v}{d\varepsilon_\gamma} = \frac{dh/dD}{dx/dD} = \frac{dh}{dx} \tag{6}$$

where ψ is the shear dilation angle of the soil; $d\varepsilon_v$ is the volume strain increment; d_γ is the shear strain increment; h is the vertical displacement; x is the shear displacement; D is the thickness of the shear zone.

Figure 13 shows the variation of soil shear dilation rate η with different vertical loads σ and dry-wet cycles n. As the number of dry-wet cycles increases, the soils vary from shear dilation to shear contraction. By increasing the vertical consolidation stress, the number of dry-wet cycles for the change from shear dilation to shear contraction decreases. Therefore, the dry-wet cycle and vertical consolidation stress are two factors affecting the deformation of rockfill materials by shear dilation. The range analysis shows that the shear dilation of the soil is more prominently influenced by the wet-dry cycle.

As one of the basic properties of soil, shear dilation is a dominant factor influencing the deformation and damage properties of soil (Zhang et al., 2016). Soil shear dilation depends on the soil particle composition and the interaction between the particles. The dry-wet cycle intensifies the disintegration of the block particles in the soil, and the structural characteristics of the soil are constantly changing, with different shear dilations. When the number of dry-wet cycles is 0, the block particles are not disintegrated in water, and the friction between the block particles causes the gradual hollowing of some particles. At this time, the soil volume continuously increases, and the deformation caused by shear dilation significantly intensifies until the soil is damaged by yielding deformation. With the intensification of dry-wet cycles, the block particles are continuously disintegrated by water, and the dense skeleton structure of the soil is seriously damaged. Coupled with the stress concentration during shear deformation, the pores between the grains are gradually closed by pressure, reducing the volume of the soil. At this time, most fine particles formed by disintegration are directionally arranged along the shear surface. With the increasing shear stress in the soil, the soil body shows shear plastic flow damage.

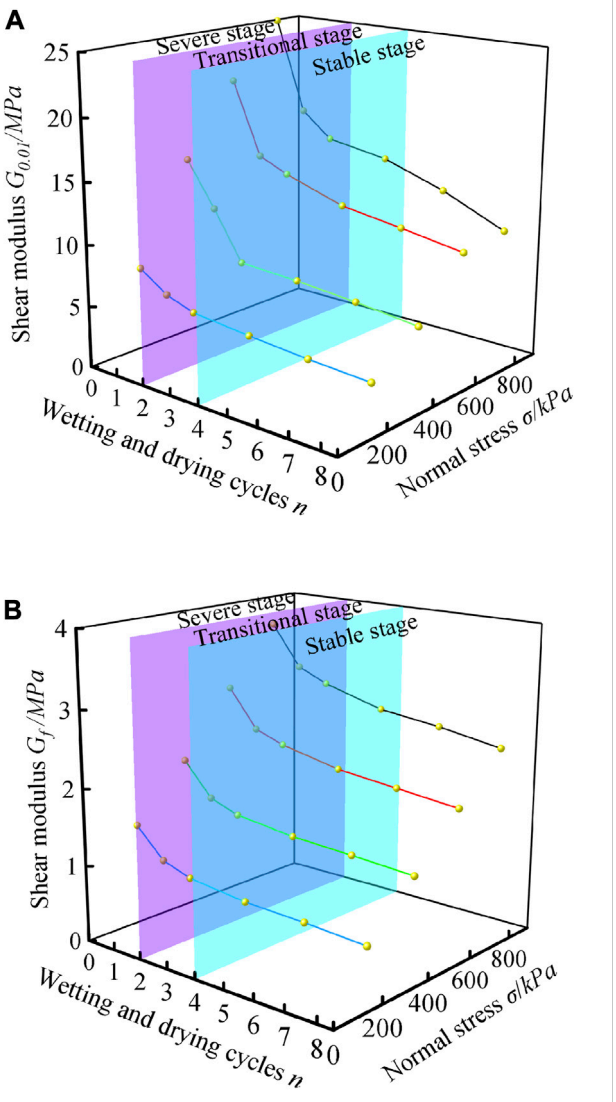

FIGURE 14
Curves of shear modulus under dry-wet cycles. **(A)** $G_{0.01}$. **(B)** G_f.

4.2.2 Shear modulus

The soil shear modulus G characterizes the ability of the soil to resist shear deformation. When shear deformation occurs in rockfill materials, the shear modulus continuously changes with the increase of shear displacement. Its value can be expressed by the slope of the tangent line at a point on the stress-shear strain curve. The shear modulus corresponding to shear strain 0.01 (shear displacement 3 mm) and shear damage (shear displacement 45 mm) are denoted as $G_{0.01}$ and G_f, respectively, and the variation of the shear modulus of rockfill materials with the accumulation of dry-wet cycles is plotted in Figure 14.

It can be seen from Figure 14 that the soil shear modulus $G_{0.01}$ is greater than G_f under the same test conditions. The reason is that during the initial stage of shear, the block stone particles in rockfill materials are closely interlocked, enhancing the rolling and friction

of the particle. The shear force required to develop a small shear deformation of the soil sample rapidly increases, and the shear modulus $G_{0.01}$ corresponding to a shear strain of 0.01 is large. During the shear damage stage, rupture occurs in the soil particle interlocking structure, resulting in a loose soil structure at the shear surface and a slow increase in shear stress. At this time, the shear modulus G_f of the soil relatively decreases. When the number of dry-wet cycles n is fixed, the soil is more densely squeezed with the increase of vertical load σ. The resistance to shear deformation is enhanced, and the soil shear modulus $G_{0.01}$ and G_f are increased. At a constant vertical load σ, the coarse particles in the soil continuously disintegrate until the disintegration is stable. The interlocking force between particles weakens, the number of fine particles arranged along the shear surface increases, and the shear deformation resistance of the soil gradually decreases and reaches a constant state. In this process, both $G_{0.01}$ and G_f exhibit the trend of first decreasing and then stabilizing.

5 Discussion

5.1 Relationship between strength degradation and disintegration characteristics

X-ray diffraction analysis shows that the argillaceous siltstone is rich in clay minerals, and the typical laminating structure of the rock microstructure is observed by a scanning electron microscope. The results indicating that the water stability of the argillaceous siltstone is poor, and it is easy to produce wet disintegration when it encounters water. After two dry-wet cycles, the argillaceous siltstone collapsed sharply, and the coarse particle content decreased from 100% before the test to 40.7%. After four dry-wet cycles, the disintegration rate of coarse particles slowed down and the content of coarse particles is 26.5%. After eight dry-wet cycles, it is difficult for coarse particles to disintegrate again and the content of coarse particles is 19.7%.

The strength deterioration of argillaceous siltstone rockfill also has the similar characteristics under the corresponding dry-wet cycle shear tests. When the dry-wet cycles are repeated twice, the coarse particles immersed in water to produce strong disintegration, the number of interlocking coarse particles decreased, and the shear hardening characteristics of the soil weakened. The deterioration of soil shear strength increases rapidly, and the deterioration reaches 38.01% for the soil sample with a normal load of 200 kPa. The soil cohesion decreases by 82.91% and the internal friction angle decreases by 7.97%. When the dry-wet cycles are repeated four times, the coarse particles in the soil are fully disintegrated, and the content of fine particles increased sharply. The occlusion and rolling friction of coarse particles in the shear deformation gradually disappeared, and the shear stress of soil increased slowly and tended to be stable, and the plastic flow trend began to appear. The deterioration of soil shear strength changes little, and the deterioration of the soil sample with normal load of 200 kPa is 44.52%. The soil cohesion decreases by 86.71% and the internal friction angle decreases by 13.29%. When the dry-wet cycles are repeated eight times, the soil showed plastic flow characteristics and weak stress softening phenomenon after shear yield. Because the coarse particle disintegration is basically stable, the shear strength deterioration of soil is relatively small. Taking the soil sample with 200 kPa normal load as an example, the deterioration only increased from 44.52% to 50.61% after four to eight dry-wet cycles. The soil cohesion decreases by 89.87% and the internal friction angle decreases by 18.94%.

By comparing and analyzing the results of disintegration test and strength deterioration test, it is not difficult to find that the shear strength characteristics of argillaceous siltstone rockfill under dry-wet cycles are mainly caused by wet disintegration of coarse particles in the rockfill, and the content of fine particles increases sharply. With the increase of the number of dry-wet cycles, the proportion of coarse and fine particles in the soil has changed significantly, and the skeleton structure of the soil has also changed. The coarse particles disintegrate with water, the content of fine particles is increasing, and the interlocking and rolling friction of the coarse particles are gradually weakened, which leads to the deterioration of the shear strength of the soil.

5.2 Degradation mechanism of the shear strength

The shear strength of the rockfill material is composed of the apparent cohesion and friction strength of the soil (Yang et al., 2021). The apparent cohesion reflects the adhesion degree of fine particles in the soil and the interlocking strength of coarse particles. The friction strength is a macroscopic representation of the frictional interaction of soil particles on the shear surface and the degree of directional particle arrangement. Under dry-wet cycles, the block particles in rockfill materials soften and disintegrate, the bound water between fine particles thickens, and the directional arranged fine particles on the shear surface significantly increase, resulting in the continuous deterioration of soil shear strength. The meso-mechanism of shear strength deterioration of rockfill materials under dry-wet cycles is shown in Figure 15.

Figure 15A shows the shear surface characteristics of soil samples under different dry-wet cycles. Compared with the shear surface of the soil sample after zero dry-wet cycle, the coarse particles on the shear surface after twice dry-wet cycles decreases significantly, and there is phenomenon of coarse particle breakage. After four times dry-wet cycles, the fine particles in the shear surface increased significantly, the occlusion of coarse particles decreased, and the shear surface is unsmooth. After eight times dry-wet cycles, only a small number of coarse particles are distributed on the shear surface. The shear surface is flat and smooth, and no trace of the occlusion and rolling friction of coarse particles is observed.

Figure 15B illustrates the deterioration of the apparent cohesion of the rockfill material under dry-wet cycles. It can be seen that disintegration occurs when the argillaceous siltstone rockfill material is exposed to water. The clay particles formed by disintegration are dissociated and negatively charged by water. After forming an electric field, the cations in the aqueous solution are tightly adsorbed on the surface of the clay particles through the electric field attraction to form a bound water membrane, exerting a certain bonding effect between the clay particles. However, after multiple wet-dry cycles, the coarse particles in the soil material are continuously wetted and cracked, significantly increasing the

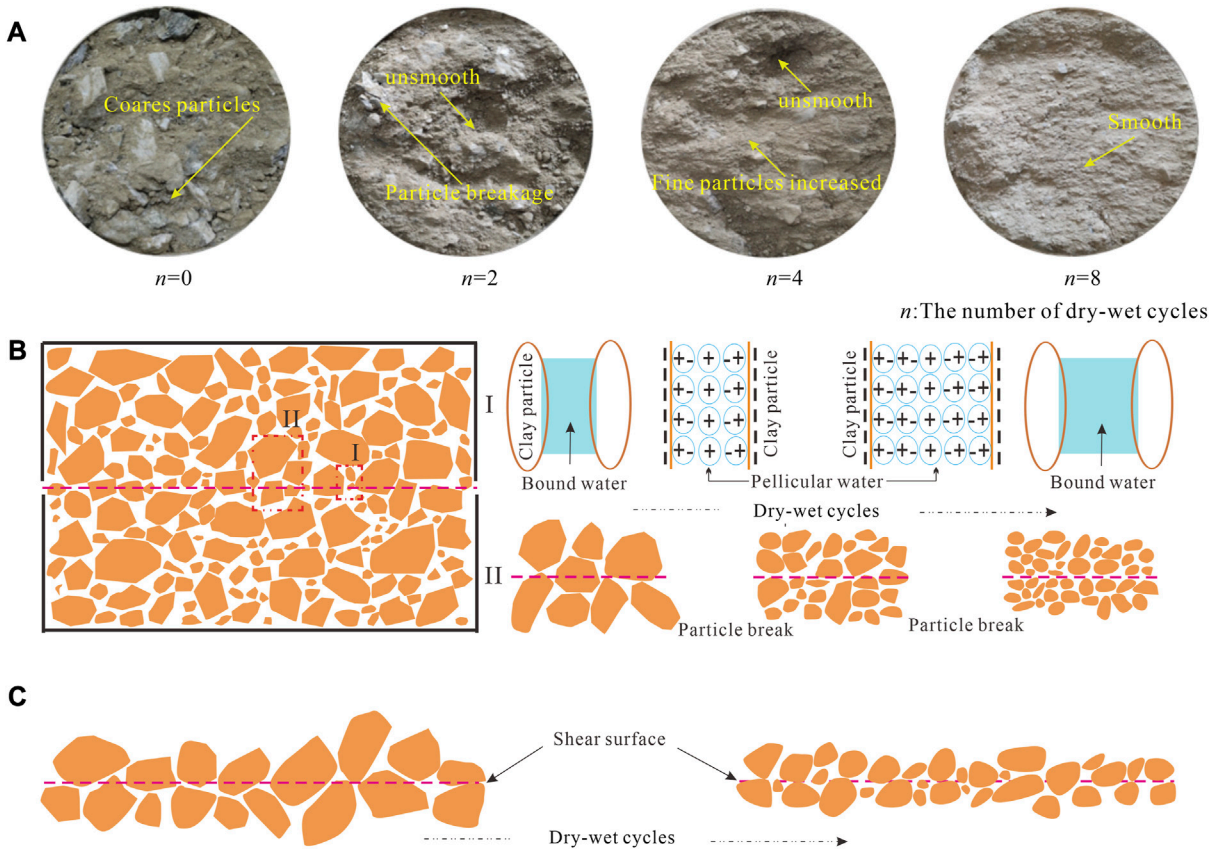

FIGURE 15
Schematic diagram of deterioration mechanism of shear strength of rockfill materials. **(A)** Shear surface of soil sample under different dry-wet cycles. **(B)** Deterioration of apparent cohesion. **(C)** Deterioration of friction strength.

number of clay particles. These particles are bound to each other through the bound water, and repeated immersion in the wetting environment thickens the bound water membrane between them. The electric field attraction is insufficient to overcome the gravitational water flow, weakening the binding strength between soil particles. Furthermore, the dry-wet cycles accelerate the shrinkage-expansion deformation of clay-rich mineral particles, with an increasing number of internal fractures. In the alternating changes of dry and wet environments, these fractures gradually open, widen, deepen, and penetrate. As a result, the disintegration of block particles continuously occurs, and the particle edges are gradually smoothed with increased roundness. The interlocking effect between particles continuously weakens, and the apparent cohesion of the soil body further deteriorates.

Figure 15C illustrates the particle distribution characteristics on the shear surface of the rockfill material under dry-wet cycles. It can be seen that under dry-wet cycles, the coarse particles are wetted and disintegrated, the number of fine particles significantly increases, the roundness of soil particles increases, and the interlocking friction between soil particles decreases significantly due to the decrease in particle size. In addition, the frictional impedance effect of the soil is weakened by the increasing number of fine particles directionally arranged on the shear surface. Due to the alternating dry and wet actions, cracks and defects sprout inside the block before the particle disintegration is completed. As a result, the soil can hardly form a stable bearing skeleton structure, and its friction strength is significantly weakened.

5.3 Analysis of the experimental limitations and sources of error

In the existing dry-wet cycle shear tests, soil material is mostly dipped and dried on the outside of the test machine and then filled into the test machine when a certain number of cycles. This test method is usually inconsistent with the stress state of soil in nature and ignores the consolidation stress condition of soil. This study realizes the dry-wet cycle process of the soil in the test machine, which can truly reflect the consolidation stress state of soil, thus avoiding the disturbance of soil structure during the preparation of the soil sample after the dry-wet circulation. Therefore, the test method is innovative. However, the direct shear test in this study still has some unavoidable experimental limitations and sources of error.

On the one hand, the shear surface of the soil in the indoor direct shear test is artificially fixed and decreases with shear, the shear zone is limited to the upper and lower shear box openings and the particles cannot be fully deformed. These defects in the test apparatus inevitably have an impact on the test results. On the other hand, as with existing indoor geotechnical test equipment for coarse-grained soils, the size of the test machine is limited by the

inability to carry out shear tests on full-scale graded soils. The maximum particle size allowed in the direct shear test is 60mm, which is very different from the maximum particle size in the field. Therefore, the test results can only reflect the change law of shear strength of soil and reveal the internal mechanism of action, but cannot reflect the real mechanical properties and strength index results of soil.

In order to eliminate the influence of artificial fixed shear surface on the test results, the laminated shear test should be carried out, that is, multiple shear planes are set in the test apparatus, and the shear strength characteristics of the soil are revealed by analyzing the most unfavorable shear weak plane in the soil. In addition, in order to eliminate the scale effect of the test soil material, it is necessary to carry out full scale *in-situ* test. *In-situ* tests require improved accuracy of data acquisition and stability of pressure control. This aspect of the research will be progressively improved in subsequent research work.

6 Conclusion

Based on the disintegration resistance test and dry-wet cycle shear test of the argillaceous siltstone rockfill materials, this paper reveals that the characteristics of wet disintegration and shear strength deterioration of rockfill materials, and analyzes the strength deterioration mechanism of rockfill materials from the meso-structure. The main conclusions are provided as follows.

(1) The argillaceous siltstone is rich in clay minerals, with a content of over 60%, and disintegrates strongly when exposed to water. The disintegration degree of argillaceous siltstone has the characteristics of three stages with the accumulation of dry-wet cycles. The massive disintegration stage ($n \leq 2$) has a significant reduction in coarse grain content and a significant increase in disintegrate content, the transitional stage ($2 < n \leq 4$) has a slower disintegration rate of coarse grains in water, the stabilization stage ($n > 4$) is difficult to produce further fractures of coarse grains and the disintegrate content almost ceases to change.
(2) The dry-wet cycle change condition of rockfill material inside shear testing machine is realized. With the accumulation of dry-wet cycles, the rockfill material experiences deformation from shear dilation to shear contraction. The shear damage of rockfill material gradually progresses from strain hardening to shear plastic flow, exhibiting a slight stress softening characteristic. Both soil cohesion and internal friction angle show the trend of first decreasing and then stabilizing under dry-wet cycles. However, the deterioration degree of cohesion is significantly greater than that of the internal friction angle.
(3) The weakening of the apparent cohesion and friction strength of soil are the main reasons for the shear strength deterioration of rockfill material in the alternating dry-wet cycle. The fine particles are bound to each other through the bound water, and repeated immersion in the wetting environment thickens the bound water membrane between them. The electric field attraction is insufficient to overcome the gravitational water flow, weakening the binding strength between soil particles. Meanwhile, the coarse particles are wetted and disintegrated, the number of fine particles significantly increases. The roundness of the particles on the shear surface increases, and the number of directionally arranged particles increases, weakening the frictional impedance effect of the soil.

Data availability statement

The original contributions presented in the study are included in the article/Supplementary Material, further inquiries can be directed to the corresponding author.

Author contributions

Conceptualization, JD, XS; validation, CL, GF; supervision, JD; writing—original draft preparation, JD, XS, and CL; writing—review and editing, WZ and GF. All authors contributed to the article and approved the submitted version.

Funding

This work was supported by the Special Basic Cooperative Research Programs of Yunnan Provincial Undergraduate University's Association (202001BA070001-066, 202101BA070001-137), Basic Research Project of Yunnan Province of China (202101AT070144), and Talent Introduction Program of Kunming University (XJ20220015).

Conflict of interest

The authors declare that the research was conducted in the absence of any commercial or financial relationships that could be construed as a potential conflict of interest.

Publisher's note

References

Abbas, M. F., Shaker, A. A., and Al-Shamrani, M. A. (2023). Hydraulic and volume change behaviors of compacted highly expansive soil under cyclic wetting and drying. *J. Rock Mech. Geotech.* 15 (2), 486–499. doi:10.1016/J.JRMGE.2022.05.015

Ahmed, S. S., Martinez, A., and DeJong, J. T. (2023). Effect of gradation on the strength and stress-dilation behavior of coarse-grained soils in drained and undrained triaxial compression. *J. Geotech. Geoenviron.* 149(5), 04023019. doi:10.1061/JGGEFK.GTENG-10972

Cavarretta, I., Coop, M., and O'Sullivan, C. (2010). The influence of particle characteristics on the behaviour of coarse grained soils. *Geotechnique* 60 (6), 413–423. doi:10.1680/geot.2010.60.6.413

Chen, X. B., Jia, Y., and Zhang, J. S. (2018). Stress-strain response and dilation of geogrid-reinforced coarse-grained soils in large-scale direct shear tests. *Geotech. Test. J.* 41 (3), 20160089–20160610. doi:10.1520/GTJ20160089

Cook, M. E., Brook, M. S., Hamling, I. J., Cave, M., Tunnicliffe, J. F., and Holley, R. (2023). Investigating slow-moving shallow soil landslides using Sentinel-1 InSAR data in Gisborne, New Zealand. *Landslides* 20, 427–446. doi:10.1007/s10346-022-01982-9

Huang, M. S., Yao, Y. P., Yin, Z. Y., Liu, E. L., and Lei, H. Y. (2016). An overview on elementary mechanical behaviors, constitutive modeling and failure criterion of soils. *China Civ. Eng. J.* 49 (7), 9–35. doi:10.15951/j.tmgcxb.2016.07.002

Jia, H. L., Wang, T., Xiang, W., Tan, L., Shen, Y. J., and Yang, G. S. (2018). Influence of water content on the physical and mechanical behaviour of argillaceous siltstone and some microscopic explanations. *Chin. J. Rock Mech. Eng.* 37 (7), 1618–1628. doi:10.13722/j.cnki.jrme.2017.1037

Jia, Y. F., Yao, S. E., and Chi, S. C. (2019). Wetting of coarse-grained soil under equal stress ratio path. *Chin. J. Geotech. Eng.* 41 (4), 648–654. doi:10.11779/CJGE201904007

Li, S. Y., He, Z. L., Zhu, P., Mei, L. X., Zeng, S. J., and Wang, S. W. (2022). Experimental study on the triaxial compression properties of coarse-grained filling soil under drying–wetting cycles. *Geofluids* 2022, 1–14. doi:10.1155/2022/1452916

Li, Z., Liu, L. L., Yan, S. H., Zhang, M. K., and Xie, Y. L. (2019). Properties of microscopic particle morphology and particle contact of renewable construction waste mixtures. *Constr. Build. Mat.* 207, 190–205. doi:10.1016/j.conbuildmat.2019.02.135

Luo, Y. H., Zhu, C. L., and Li, J. D. (2003). Research for distortion-destruction mechanism of slopes of red strata in Yunnan province and their hazard control. *Rock Soil Mech.* 24 (5), 836–839. doi:10.16285/j.rsm.2003.05.037

Nguyen, H. B. K., Rahman, M. M., and Karim, M. R. (2023). Effect of soil anisotropy and variability on the stability of undrained soil slope. *Front. Built Environ.* 9, 1117858. doi:10.3389/fbuil.2023.1117858

Oliveira, J., Cássaro, F., and Pires, L. (2021). Estimating soil porosity and pore size distribution changes due to wetting-drying cycles by morphometric image analysis. *Soil. till. Res.* 205, 104814. doi:10.1016/j.still.2020.104814

Pan, Y., Wu, G., Zhao, Z. M., and He, L. (2020). Analysis of rock slope stability under rainfall conditions considering the water-induced weakening of rock. *Comput. Geotech.* 128, 103806. doi:10.1016/j.compgeo.2020.103806

Peng, M., and Zhang, L. M. (2012). Breaching parameters of landslide dams. *Landslides* 9, 13–31. doi:10.1007/s10346-011-0271-y

Pham, T., Zaman, M. W., and Vu, T. (2022). Modeling triaxial testing with flexible membrane to investigate effects of particle size on strength and strain properties of cohesion less soil. *Transp. Infrastruct. Geotech.* 9, 417–441. doi:10.1007/s40515-021-00167-6

Rasul, J. M., Ghataora, G. S., and Burrow, M. P. N. (2018). The effect of wetting and drying on the performance of stabilized subgrade soils. *Transp. Geotech.* 14, 1–7. doi:10.1016/j.trgeo.2017.09.002

Silvani, C., Bonelli, S., Philippe, P., and Desoyer, T. (2008). Buoyancy and local friction effects on rockfill settlements: a discrete modelling. *Comput. Math. Appl.* 55 (2), 208–217. doi:10.1016/j.camwa.2007.04.011

Tran, K. M., Bui, H. H., and Nguyen, G. D. (2021). Hybrid discrete-continuum approach to model hydro mechanical behavior of soil during desiccation. *J. Geotech. Geoenviron.* 147 (10), 040211. doi:10.1061/(ASCE)GT.1943-5606.0002633

Wang, G. J., Yang, C. H., Kong, X. Y., and Liu, T. N. (2012). Research on fragmentation distribution and shear strength parameters of accumulate granulae with superhigh bench dumping site. *Rock Soil Mech.* 33 (10), 3087–3092+3161. doi:10.16285/j.rsm.2012.10.017

Wang, G. J., Yang, C. H., Zhang, C., Mao, H. J., and Wang, W. (2009). Experimental research on particle breakage and strength characteristics of rock and soil materials with different coarse-grain contents. *Rock Soil Mech.* 30 (12), 3649–3654. doi:10.16285/j.rsm.2009.12.031

Wei, H., Wu, D. Y., Wu, H. G., Tang, L., Wang, S., and Sun, H. (2023). Coordinated evolution and mechanism characteristics of the tunnel-landslide system under rainfall conditions. *Eng. Fail. Anal.* 146, 107118. doi:10.1016/j.engfailanal.2023.107118

Wei, S., and Zhu, J. G. (2006). Study on wetting breakage of coarse-grained materials in triaxial test. *Chin. J. Rock Mech. Eng.* 25 (6), 1252–1258. doi:10.1016/S1872-1508(06)60035-1

Wen, C. P., and Yuan, X. Q. (2022). Hyperbolic consolidation creep model of weathered red sandstone coarse-grained soil under the wet and dry cycles conditions. *Geotech. Geol. Eng.* 40, 5103–5113. doi:10.1007/s10706-022-02202-w

Wu, E. L., Zhu, J. G., Chen, G., and Wang, L. (2020). Experimental study of effect of gradation on compaction properties of rockfill materials. *Bull. Eng. Geol. Environ.* 79, 2863–2869. doi:10.1007/s10064-020-01737-7

Wu, E. L., Zhu, J. G., He, S. B., and Peng, W. M. (2021). A stress dilatancy relationship for coarse-grained soils incorporating particle breakage. *Granul. Matter.* 24 (1), 4. doi:10.1007/S10035-021-01147-W

Wu, Y. K., Shi, K. J., Han, Y., Han, T., Yu, J. L., and Li, D. D. (2021). Experimental study on strength characteristics of expansive soil improved by steel slag powder and cement under dry–wet cycles. *Iran. J. Sci. Technol. Trans. Civ. Eng.* 45, 941–952. doi:10.1007/s40996-020-00473-y

Xu, X. T., Shao, L. J., Huang, J. B., Xiang, X., Liu, D. Q., Xian, Z. X., et al. (2021). Effect of wet-dry cycles on shear strength of residual soil. *Soils Found.* 61 (3), 782–797. doi:10.1016/J.SANDF.2021.03.001

Xue, Y., Liang, X., Li, X., Wang, S. H., Ma, Z. Y., Zhang, S. W., et al. (2023). Influence mechanism of brine-gas two-phase flow on sealing property of anisotropic caprock for hydrogen and carbon energy underground storage. *Int. J. Hydrogen. Energy* 48 (30), 11287–11302. doi:10.1016/j.ijhydene.2022.05.173

Xue, Y., Liu, S., Chai, J. R., Liu, J., Ranjith, P. G., Cai, C. Z., et al. (2023). Effect of water-cooling shock on fracture initiation and morphology of high-temperature granite: application of hydraulic fracturing to enhanced geothermal systems. *Appl. Energ* 337, 120858. doi:10.1016/j.apenergy.2023.120858

Yang, Z. P., Zhao, Y. L., Hu, Y. X., Li, S. Q., Lei, X. D., and Li, X. Y. (2021). Effect of the strength of rock blocks on the shear characteristics of soil-rock mixtures. *Chin. J. Rock Mech. Eng.* 40 (4), 814–827. doi:10.13722/j.cnki.jrme.2020.0488

Yuan, J., Liu, Z. H., Hu, G. X., and Fang, Y. G. (2018). Experimental analysis of the influence of soil composition on strength characteristics. *Soil. Mech. Found. Eng.* 55, 325–332. doi:10.1007/s11204-018-9544-y

Zeng, L., Luo, J. T., Liu, J., Gao, Q. F., and Bian, H. B. (2021). Disintegration characteristics and mechanisms of carbonaceous mudstone subjected to load and cyclic drying–wetting. *J. Mat. Civ. Eng.* 33 (8), 04021195. doi:10.1061/(ASCE)MT.1943-5533.0003817

Zhang, B. Y., Zhang, J. H., and Sun, G. L. (2015). Deformation and shear strength of rockfill materials composed of soft siltstones subjected to stress, cyclical drying/wetting and temperature variations. *Eng. Geol.* 190, 87–97. doi:10.1016/j.enggeo.2015.03.006

Zhang, G., Wang, G., Yin, Z. Y., and Yang, Z. X. (2016). A critical review on the research of fundamental behavior and constitutive relationship of the soil. *China Civ. Eng. J.* 53 (2), 105–118. doi:10.15951/j.tmgcxb.2020.02.009

Zhang, H. J., Adoko, A. C., Meng, Z. J., Wang, H., and Jiao, Y. Y. (2017). Mechanism of the mudstone tunnel failures induced by expansive clay minerals. *Geotech. Geol. Eng.* 35 (1), 263–275. doi:10.1007/s10706-016-0102-y

Zhang, J. Z., and Zhou, X. P. (2020). AE event rate characteristics of flawed granite: from damage stress to ultimate failure. *Geophys. J. Int.* 222 (2), 795–814. doi:10.1093/gji/ggaa207

Zhang, J. Z., Zhou, X. P., Zhou, L. S., and Berto, F. (2019). Progressive failure of brittle rocks with non-isometric flaws: insights from acousto-optic-mechanical (AOM) data. *Fatigue Fract. Eng. Mater Struct.* 42 (8), 1787–1802. doi:10.1111/ffe.13019

Zhou, X., Ma, G., and Zhang, Y. D. (2019). Grain size and time effect on the deformation of rockfill dams: a case study on the shuibuya CFRD. *Geotechnique* 69 (7), 606–619. doi:10.1680/jgeot.17.P.299

Zhou, X. P., Cheng, H., and Feng, Y. F. (2014). An experimental study of crack coalescence behaviour in rock-like materials containing multiple flaws under uniaxial compression. *Rock Mech. Rock Eng.* 47 (6), 1961–1986. doi:10.1007/s00603-013-0511-7

Zhou, X. P., Lian, Y. J., Wong, L. N. Y., and Berto, F. (2018). Understanding the fracture behavior of brittle and ductile multi-flawed rocks by uniaxial loading by digital image correlation. *Eng. Fract. Mech.* 199, 438–460. doi:10.1016/j.engfracmech.2018.06.007

Zhou, X. P., Wang, Y. T., Zhang, J. Z., and Liu, F. N. (2019). Fracturing behavior study of three-flawed specimens by uniaxial compression and 3D digital image correlation: sensitivity to brittleness. *Rock Mech. Rock Eng.* 52 (3), 691–718. doi:10.1007/s00603-018-1600-4

Zhou, X. P., Zhang, J. Z., Qian, Q. H., and Niu, Y. (2019). Experimental investigation of progressive cracking processes in granite under uniaxial loading using digital imaging and AE techniques. *J. Struct. Geol.* 126, 129–145. doi:10.1016/j.jsg.2019.06.003